Hindawi Publishing Corporation
Advances in Optics
Volume 2014, Article ID 942750, 5 pages
http://dx.doi.org/10.1155/2014/942750

Research Article

Self-Focusing of Hermite-Cosh-Gaussian Laser Beams in Plasma under Density Transition

Manzoor Ahmad Wani and Niti Kant

Department of Physics, Lovely Professional University, Phagwara, Punjab 144411, India

Correspondence should be addressed to Manzoor Ahmad Wani; manzoorphysics@gmail.com

Received 16 June 2014; Accepted 9 September 2014; Published 29 September 2014

Academic Editor: Kim Fook Lee

Copyright © 2014 M. A. Wani and N. Kant. This is an open access article distributed under the Creative Commons Attribution License, which permits unrestricted use, distribution, and reproduction in any medium, provided the original work is properly cited.

Self-focusing of Hermite-Cosh-Gaussian (HChG) laser beam in plasma under density transition has been discussed here. The field distribution in the medium is expressed in terms of beam-width parameters and decentered parameter. The differential equations for the beam-width parameters are established by a parabolic wave equation approach under paraxial approximation. To overcome the defocusing, localized upward plasma density ramp is considered, so that the laser beam is focused on a small spot size. Plasma density ramp plays an important role in reducing the defocusing effect and maintaining the focal spot size up to several Rayleigh lengths. To discuss the nature of self-focusing, the behaviour of beam-width parameters with dimensionless distance of propagation for various values of decentered parameters is examined by numerical estimates. The results are presented graphically and the effect of plasma density ramp and decentered parameter on self-focusing of the beams has been discussed.

1. Introduction

The self-focusing of laser beams in nonlinear optical media is a fascinating topic which has inspired theoretical and experimental interest [1–3]. In self-focusing and self-phase modulation of Cosh-Gaussian laser beam in magnetoplasma using variational approach, it is found that the decentered parameter along with absorption coefficient plays a key role in the nature of self-focusing/defocusing of the beam [4]. However in the propagation of a Cos-Gaussian beam in a kerr medium, it is found that although the RMS beam width broadens, the central parts of the beam give rise to an initial radial compression and a significant redistribution during propagation. The partial collapse of central part of the beam appears while the RMS beam width still increases or remains constant. It is further observed that the Cos-Gaussian beam eventually converts into a Cosh-Gaussian type beam in a kerr medium with low and moderate power [5]. In self-focusing of Cosh-Gaussian laser beam in plasma with weak relativistic and ponderomotive regime, it is observed that a large value of absorption level weakens the self-focusing effect in the absence of decentered parameter. However, oscillatory self-focusing takes place for a higher value of decentered parameter, $b = 1$, and all curves are seen to exhibit sharp self-focusing effect for $b = 2$ [6]. In ponderomotive self-focusing of a short laser pulse under plasma density ramp, the pulse acquires a minimum spot size. As the laser propagates through the density ramp region, it sees a slowly narrowing channel. In such a case the oscillation amplitude of the spot size shrinks, while its frequency increases. Therefore, the laser pulse propagating in a plasma density ramp tends to become more focused. If there is no density ramp, the laser pulse is defocused due to the dominance of the diffraction effect. As the plasma density increases, self-focusing effect becomes stronger. Similarly as in case of no density ramp, the beam-width parameter does not increase much. After several Rayleigh lengths, the beam-width parameter attains a minimum value and maintains it for a long distance. Consequently, the self-focusing effect is enhanced and the laser pulse is more focused [7].

Nanda et al. [8] while studying the enhanced relativistic self-focusing of Hermite-Cosh Gaussian laser beam in plasma under density transition observed that the proper selection of decentered parameter and presence of density transition

results stronger self-focusing of laser beam. In self-focusing of Hermite-Cosh Gaussian laser beam in a magnetoplasma with a ramp density profile, the authors concluded that the presence of plasma density ramp and magnetic field enhances the self-focusing effect to a greater extent [9]. The proper selection of decentered parameter was very much sensitive to self-focusing [10]. However in studying the self-focusing of Hermite-Gaussian laser beams in plasma under plasma density ramp by Kant et al. [11] the authors found that the effect of plasma density ramp and initial intensity of the laser beam are important and play a vital role in laser plasma interaction and hence in strong self-focusing of laser beam.

Recently, a new laser beam, called the Hermite-Cosh-Gaussian (HChG) beam, has been studied extensively and it has been found that such beams can be generated in the laboratory by the superposition of two decentered Hermite-Gaussian beams as Cosh-Gaussian ones [12]. In this paper, we mainly study the self-focusing of HChG laser beams propagating in underdense plasma under plasma density ramp of the form $n(\xi) = n_0 \mathrm{Tan}(\xi/d)$ by a ponderomotive mechanism. Analytical formulas for HChG beams are derived and results are discussed.

2. Theoretical Considerations

2.1. Field Distribution of HChG Beams. We employed the propagation of HChG laser beam along z-axis in the plasma with the field distribution in the following form:

$$E(r,z) = \frac{E_0}{2f} H_m\left(\frac{\sqrt{2}r}{r_0 f}\right)\exp\left(\frac{b^2}{4}\right) \times \left\{\exp\left[-\left(\frac{r}{r_0 f}+\frac{b}{2}\right)^2\right] + \exp\left[-\left(\frac{r}{r_0 f}-\frac{b}{2}\right)^2\right]\right\}, \tag{1}$$

where m is the mode index associated with the Hermite Polynomial H_m, r_0 is the waist width of Gaussian amplitude distribution, b is the decentered parameter, r is the radial coordinate, E_0 is the amplitude of Gaussian beams for the central position at $r = z = 0$, $A_0(r,z)$ is the amplitude of HChG beams in cylindrical coordinates, and f is the dimensionless beam-width parameter, which is a measure of both axial intensity and width of the beam.

2.2. Nonlinear Dielectric Constant. Further, we consider propagation of HChG laser beam in a nonlinear medium characterized by dielectric constant of the form

$$\varepsilon = \varepsilon_0 + \Phi\left(EE^*\right) \tag{2}$$

with $\varepsilon_0 = 1 - \omega_p^2/\omega^2$ and $\omega_p^2 = 4\pi n(\xi)e^2/m$.

With

$$n(\xi) = n_0 \mathrm{Tan}\left(\frac{\xi}{d}\right), \qquad \xi = \frac{z}{R_d},$$
$$\varepsilon_0 = 1 - \left(\frac{\omega_{p0}^2}{\omega^2}\right)\mathrm{Tan}\left(\frac{\xi}{d}\right), \qquad \omega_{p0}^2 = \frac{4\pi n_0 e^2}{m}, \tag{3}$$

where ε_0 and Φ represent the linear and nonlinear parts of dielectric constant, respectively, ω_p is plasma frequency, e is the electronic charge, m is the electron mass, n_0 is the equilibrium electron density, R_d is the diffraction length, ξ is the normalized propagation distance, and d is a dimensionless adjustable parameter.

Now, in case of collision-less plasma, the nonlinearity in the dielectric constant is mainly due to ponderomotive force and the nonlinear part of dielectric constant is given by

$$\Phi\left(AA^*\right) \approx \left(\frac{1}{2}\right)\varepsilon_2 A_0^2 \tag{4}$$

with

$$\varepsilon_2 = 2\left(\frac{\omega_p^2}{\omega^2}\right)\alpha; \quad \alpha = \frac{e^2 M}{6m^2\omega^2 K_b T_0}, \tag{5}$$

where M is the mass of scatterer in the plasma, ω is the frequency of laser used, K_b is the Boltzmann constant, and T_0 is the equilibrium plasma temperature.

3. Self-Focusing

The wave equation governing the propagation of laser beam may be written as follows:

$$\nabla^2 E + \left(\frac{\omega^2}{c^2}\right)\varepsilon E + \nabla\left(\frac{E\nabla\varepsilon}{\varepsilon}\right) = 0. \tag{6}$$

The last term of (6) on left-hand side can be neglected provided that $k^{-2}\nabla^2(\ln\varepsilon) \ll 1$, where "$k$" represents the wave number. Thus,

$$\nabla^2 E + \left(\frac{\omega^2}{c^2}\right)\varepsilon E = 0. \tag{7}$$

This equation is solved by employing Wentzel-Kramers-Brillouin (WKB) approximation. Employing the WKB approximation, (7) reduces to a parabolic wave equation as follows:

$$\frac{i\omega}{c}\left(2\sqrt{1-\frac{\omega_{p0}^2}{\omega^2}\mathrm{Tan}\left(\frac{z}{dR_d}\right)} - \frac{\left(\omega_{p0}^2/\omega^2\right) z\mathrm{Sec}^2\left(z/dR_d\right)}{dR_d\sqrt{1-\left(\omega_{p0}^2/\omega^2\right)\mathrm{Tan}\left(z/dR_d\right)}}\right)\left(\frac{\partial A}{\partial z}\right) - \frac{\left(\omega_{p0}^2/\omega^2\right) A\mathrm{Sec}^2\left(z/dR_d\right)}{dR_d\sqrt{1-\left(\omega_{p0}^2/\omega^2\right)\mathrm{Tan}\left(z/dR_d\right)}}$$

$$
\begin{aligned}
&-\frac{\left(\omega_{p0}^2/\omega^2\right) Az\mathrm{Sec}^2\left(z/dR_d\right)}{d^2R_d^2\sqrt{1-\left(\omega_{p0}^2/\omega^2\right)\mathrm{Tan}\left(z/dR_d\right)}} \\
&\times\left(\mathrm{Tan}\left(\frac{z}{dR_d}\right)+\frac{\left(\omega_{p0}^2/\omega^2\right)\mathrm{Sec}^2\left(z/dR_d\right)}{4\left(1-\left(\omega_{p0}^2/\omega^2\right)\mathrm{Tan}\left(z/dR_d\right)\right)}\right) \\
&=\frac{\omega^2}{c^2}\left(\frac{\left(\omega_{p0}^2/\omega^2\right) Az\mathrm{Sec}^2\left(z/dR_d\right)}{dR_d}\right. \\
&\qquad\left.-\frac{\left(\omega_{p0}^2/\omega^2\right)^2 Az^2\mathrm{Sec}^4\left(z/dR_d\right)}{4d^2R_d^2\left(1-\left(\omega_{p0}^2/\omega^2\right)\mathrm{Tan}\left(z/dR_d\right)\right)}\right)\frac{\partial^2 A}{\partial r^2} \\
&\quad+\frac{1}{r}\frac{\partial A}{\partial r}+\frac{\omega^2}{c^2}\Phi\left(AA^*\right)A.
\end{aligned}
\tag{8}
$$

To solve (8) we express A as

$$
A=A_0\left(r,z\right)\exp\left[-iks\left(r,z\right)\right], \tag{9}
$$

where

$$
k=\frac{\omega}{c}\sqrt{1-\frac{\omega_{p0}^2}{\omega^2}\mathrm{Tan}\left(\frac{z}{dR_d}\right)}, \tag{10}
$$

where "A_0" and "S" are real functions of r and z with $S(r,z)$ as eikonal of the beam which determines convergence/divergence of the beam. Substituting for A from (9) in (8) and equating real and imaginary parts on both sides of the resulting equation, one obtains

$$
\begin{aligned}
&\frac{c^2}{\omega^2A_0}\left(\frac{\partial^2A_0}{\partial r^2}+\frac{1}{r}\frac{\partial A_0}{\partial r}\right)+\Phi\left(A_0^2\right) \\
&=\left(2\left(1-\frac{\omega_{p0}^2}{\omega^2}\mathrm{Tan}\left(\frac{z}{dR_d}\right)\right)-\frac{\omega_{p0}^2}{\omega^2}\frac{z\mathrm{Sec}^2\left(z/dR_d\right)}{dR_d}\right)\frac{\partial S}{\partial z} \\
&\quad+\left(1-\frac{\omega_{p0}^2}{\omega^2}\mathrm{Tan}\left(\frac{z}{dR_d}\right)\right)\left(\frac{\partial S}{\partial r}\right)^2 \\
&\quad-\frac{\omega_{p0}^2}{\omega^2}\frac{\mathrm{Sec}^2\left(z/dR_d\right)}{dR_d} \\
&\quad\times\left(S+z-\frac{\omega_{p0}^2}{\omega^2}\frac{z\mathrm{Sec}^2\left(z/dR_d\right)\left(S-z/2\right)}{2dR_d\left(1-\left(\omega_{p0}^2/\omega^2\right)\mathrm{Tan}\left(z/dR_d\right)\right)}\right), \\
&\left(1-\frac{\omega_{p0}^2}{\omega^2}\frac{z\mathrm{Sec}^2\left(z/dR_d\right)}{2dR_d\left(1-\left(\omega_{p0}^2/\omega^2\right)\mathrm{Tan}\left(z/dR_d\right)\right)}\right)\frac{\partial A_0^2}{\partial z} \\
&\quad+\frac{\partial S}{\partial r}\frac{\partial A_0^2}{\partial r}+\left(\frac{\partial^2S}{\partial r^2}+\frac{1}{r}\frac{\partial S}{\partial r}\right)A_0^2 \\
&\quad-\left(\frac{\omega_{p0}^2}{\omega^2}\frac{\mathrm{Sec}^2\left(z/dR_d\right)}{dR_d\sqrt{1-\left(\omega_{p0}^2/\omega^2\right)\mathrm{Tan}\left(z/dR_d\right)}}\right. \\
&\qquad\left.+\frac{\omega_{p0}^2}{\omega^2}\frac{z\mathrm{Sec}^2\left(z/dR_d\right)\mathrm{Tan}\left(z/dR_d\right)}{d^2R_d^2\sqrt{1-\left(\omega_{p0}^2/\omega^2\right)\mathrm{Tan}\left(z/dR_d\right)}}\right)A_0^2 \\
&\quad-\left(\frac{\omega_{p0}^2}{\omega^2}\right)^2\left(\frac{z\mathrm{Sec}^4\left(z/dR_d\right)}{4d^2R_d^2\left(1-\left(\omega_{p0}^2/\omega^2\right)\mathrm{Tan}\left(z/dR_d\right)\right)}\right)A_0^2 \\
&=0.
\end{aligned}
\tag{11}
$$

The solutions of (11) for a cylindrically symmetric HChG beam can be written as follows:

$$
\begin{aligned}
S&=\frac{r^2}{2}\beta\left(z\right)+\Phi\left(z\right), \\
A_0^2&=\frac{E_0^2}{4f^2}H_m^2\left(\frac{\sqrt{2}r}{r_0f}\right)\exp\left(\frac{b^2}{2}\right) \\
&\quad\times\left\{\exp\left[-2\left(\frac{r}{r_0f}+\frac{b}{2}\right)^2\right]+\exp\left[-2\left(\frac{r}{r_0f}-\frac{b}{2}\right)^2\right]\right. \\
&\qquad\left.+2\exp\left[-\left(\frac{2r^2}{r_0^2f^2}+\frac{b^2}{2}\right)\right]\right\}
\end{aligned}
\tag{12}
$$

with

$$
\beta\left(z\right)=\frac{1}{f\left(z\right)}\frac{\partial f}{\partial z}, \tag{13}
$$

where $\beta(z)$ is the inverse radius of curvature of wave front and $\Phi(z)$ is the phase shift.

Under the paraxial approximation, we have established the differential equation of the beam-width parameter for the $m=0$ mode as follows:

$$
\begin{aligned}
&\left(1-\frac{\omega_{p0}^2}{\omega^2}\mathrm{Tan}\left(\frac{\xi}{d}\right)\right)\left(\frac{6b^2}{\left(2-b^2\right)f}\right) \\
&\quad+\frac{\alpha E_0^2}{2}\left(\frac{r_0\omega}{c}\right)^2\left(\frac{\omega_{p0}^2}{\omega^2}\right)\left(1-\frac{\omega_{p0}^2}{\omega^2}\mathrm{Tan}\left(\frac{\xi}{d}\right)\right)\frac{\mathrm{Tan}\left(\xi/d\right)}{f^3} \\
&=\left[\left(\frac{\omega_{p0}^2}{\omega^2}\right)\mathrm{Tan}\left(\frac{\xi}{d}\right)+\left(\frac{\omega_{p0}^2}{\omega^2}\right)\frac{\xi\mathrm{Sec}^2\left(\xi/d\right)}{2d}-1\right]\frac{\partial^2f}{\partial\xi^2} \\
&\quad-\left[\left(\frac{\omega_{p0}^2}{\omega^2}\right)\frac{\xi\mathrm{Sec}^2\left(\xi/d\right)}{2d}\right]\frac{1}{f}\left(\frac{\partial f}{\partial\xi}\right)^2
\end{aligned}
$$

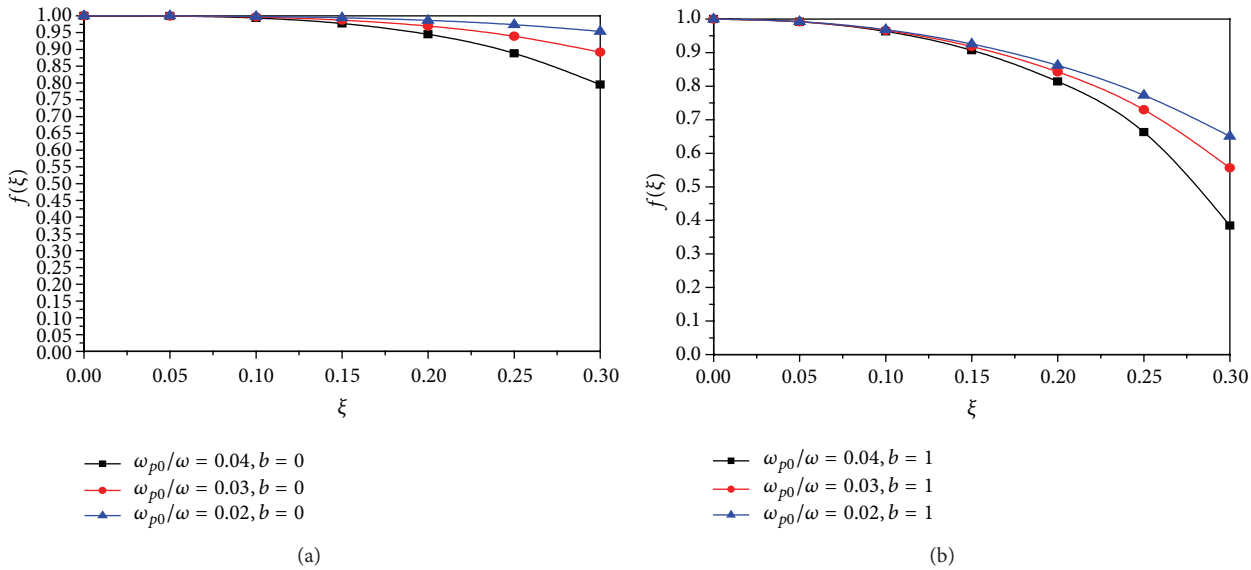

FIGURE 1: Variation of beam-width parameter with the normalised propagation distance (ξ) with a plasma density ramp. The normalized parameters are (a) $d = 5$, $\omega_{p0}/\omega = 0.02$ (blue curve), $\omega_{p0}/\omega = 0.03$ (red curve), and $\omega_{p0}/\omega = 0.04$ (black curve) at decentered parameter $b = 0$ and (b) $d = 5$, $\omega_{p0}/\omega = 0.02$ (blue curve), $\omega_{p0}/\omega = 0.03$ (red curve), and $\omega_{p0}/\omega = 0.04$ (black curve) at decentered parameter $b = 1$.

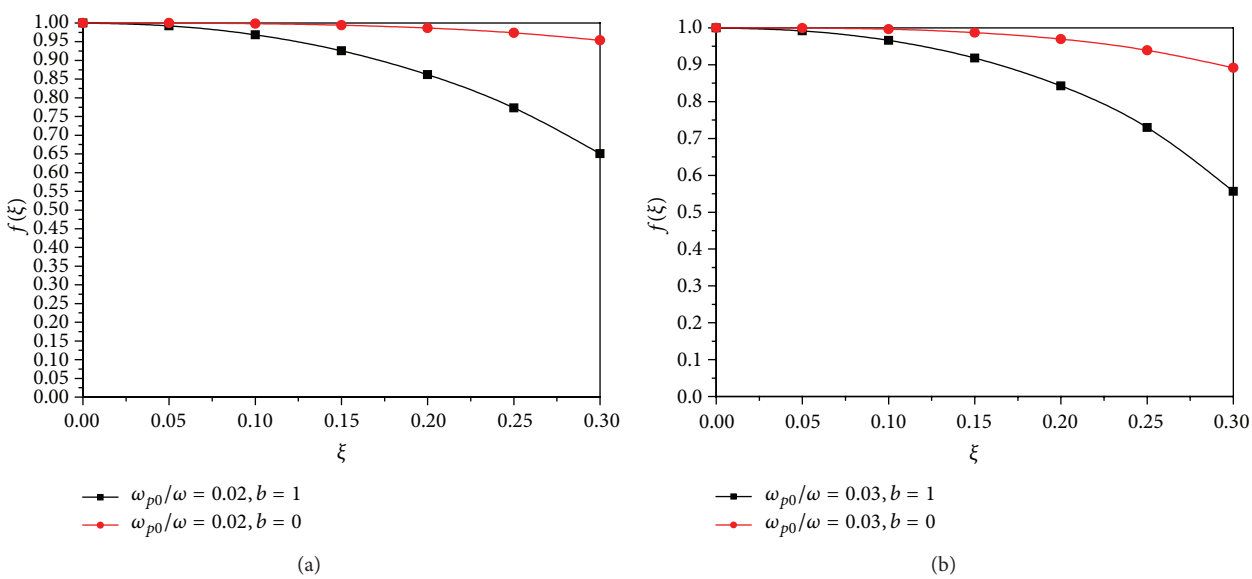

FIGURE 2: Variation of beam-width parameter with the normalised propagation distance (ξ) with a plasma density ramp. The normalized parameters are (a) $d = 5$ and decentered parameters are $b = 0$ (red curve) and $b = 1$ (black curve) at $\omega_{p0}/\omega = 0.02$ and (b) $d = 5$ and decentered parameters are $b = 0$ (red curve) and $b = 1$ (black curve) at $\omega_{p0}/\omega = 0.03$.

$$+\left(\frac{\omega_{p0}^2}{\omega^2}\right)\frac{\mathrm{Sec}^2(\xi/d)}{2d} \times\left[1-\left(\frac{\omega_{p0}^2}{\omega^2}\right)\frac{\xi\mathrm{Sec}^2(\xi/d)}{2d\left(1-\left(\omega_{p0}^2/\omega^2\right)\mathrm{Tan}(\xi/d)\right)}\right]. \tag{14}$$

Equations (14) is the required expression for beam-width parameters f.

4. Results and Discussions

For an initial plane wave front of the beam, we use the boundary conditions $f = 1$ and $\partial f/\partial\xi = 0$ at $\xi = 0$. To check the validity of the above analysis, we conduct computational simulations for solving the beam-width parameter equation. The following parameters are chosen for the purpose of numerical calculations: $\omega = 10^{14}$ rad/s, $\omega_{p0} = 5.640 \times 10^{12}$ rad/s, $r_0 = 5 \times 10^{-3}$ cm, $n_0 = 9.983 \times 10^{17}$ cm^{-3}, and $T_0 = 10^5$ K. The variation of the beam-width parameter f

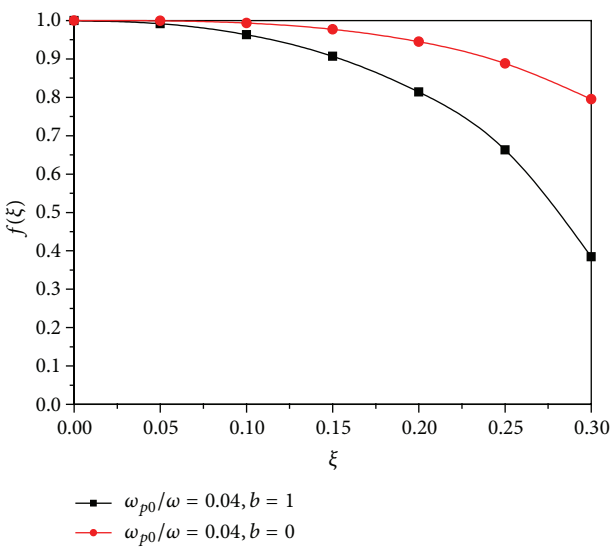

Figure 3: Variation of beam-width parameter with the normalized propagation distance (ξ) with a plasma density ramp. The normalized parameters are $d = 5$ and decentered parameters are $b = 0$ (red curve) and $b = 1$ (black curve) at $\omega_{p0}/\omega = 0.04$.

as a function of the normalized propagation distance in an underdense plasma with an upward plasma density ramp is shown in Figures 1, 2, and 3.

From the above figures, it is found that the beam gives a self-focusing effect for $b \leq 1$. It is further observed that as the plasma density increases, self-focusing becomes much stronger. Combining the results of this paper with previous studies on Gaussian beams [13, 14], we see that HChG beams give freedom to additional source parameters mode index (m) and decentered parameter (b), changing the nature of self-focusing/defocusing significantly. To overcome defocusing, localized upward plasma density ramp is introduced and it is obvious that by applying the density ramp the self-focusing effect is enhanced and the laser is more focused; that is, self-focusing becomes much stronger. Hence, the upward plasma density ramp plays an important role in enhancing laser focusing.

5. Conclusion

In the present investigation, the authors have studied the self-focusing of Hermite-Cosh-Gaussian (HChG) laser beams by considering plasma density ramp in a parabolic medium under paraxial approximation. It is observed that as both the plasma density and the decentered parameter increase, the self-focusing effect becomes stronger. However sharp self-focusing of such beams occurs for $b \leq 1$. Hence, by introducing such a density profile, a much stronger self-focusing is observed and it could produce ultrahigh laser irradiance over distances much greater than the Rayleigh length which can be used for various applications.

Conflict of Interests

The authors declare that there is no conflict of interests regarding the publication of this paper.

References

[1] R. Bingham, J. T. Mendonça, and P. K. Shukla, "Plasma based charged-particle accelerators," *Plasma Physics and Controlled Fusion*, vol. 46, no. 1, p. R1, 2004.

[2] P. Sprangle, E. Esarey, and J. Krall, "Laser driven electron acceleration in vacuum, gases, and plasmas," *Physics of Plasmas*, vol. 3, no. 5, pp. 2183–2190, 1996.

[3] D. N. Gupta and H. Suk, "Frequency chirp for resonance enhanced electron energy during laser acceleration," *Physics of Plasmas*, vol. 13, Article ID 044507, 2006.

[4] T. S. Gill, R. Kaur, and R. Mahajan, "Relativistic self-focusing and self-phase modulation of Cosh-Gaussian laser beam in magnetoplasma," *Laser and Particle Beams*, vol. 29, pp. 183–191, 2011.

[5] R. Chen, Y. Ni, and X. Chu, "Propagation of a cos-Gaussian beam in a Kerr medium," *Optics and Laser Technology*, vol. 43, no. 3, pp. 483–487, 2011.

[6] T. S. Gill, R. Mahajan, and R. Kaur, "Self-focusing of cosh-Gaussian laser beam in a plasma with weakly relativistic and ponderomotive regime," *Physics of Plasmas*, vol. 18, Article ID 033110, 2011.

[7] N. Kant, S. Saralch, and H. Singh, "Ponderomotive self-focusing of a short laser pulse under a plasma density ramp," *Nukleonika*, vol. 56, no. 2, pp. 149–153, 2011.

[8] V. Nanda and N. Kant, "Enhanced relativistic self-focusing of Hermite-cosh-Gaussian laser beam in plasma under density transition," *Physics of Plasmas*, vol. 21, no. 4, Article ID 042101, 2014.

[9] V. Nanda, N. Kant, and M. A. Wani, "Self-focusing of a Hermite-Cosh Gaussian laser beam in a magnetoplasma with ramp density profile," *Physics of Plasmas*, vol. 20, no. 11, Article ID 113109, 2013.

[10] V. Nanda, N. Kant, and M. A. Wani, "Sensitiveness of decentered parameter for relativistic self-focusing of hermite-cosh-gaussian laser beam in plasma," *IEEE Transactions on Plasma Science*, vol. 41, no. 8, pp. 2251–2256, 2013.

[11] N. Kant, M. A. Wani, and A. Kumar, "Self-focusing of Hermite-Gaussian laser beams in plasma under plasma density ramp," *Optics Communications*, vol. 285, no. 21-22, pp. 4483–4487, 2012.

[12] A. Belafhal and M. Ibnchaikh, "Propagation properties of Hermite-cosh-Gaussian laser beams," *Optics Communications*, vol. 186, no. 4–6, pp. 269–276, 2000.

[13] M. S. Sodha, A. K. Ghatak, and V. K. Tripathi, *Self Focusing of Laser Beams in Dielectrics, Semiconductors and Plasmas*, Tata-McGraw-Hill, New Delhi, India, 1974.

[14] S. Patil, M. Takale, V. Fulari, and M. Dongare, "Propagation of Hermite-cosh-Gaussian laser beams in non-degenerate germanium having space charge neutrality," *Journal of Modern Optics*, vol. 55, no. 21, pp. 3529–3535, 2008.

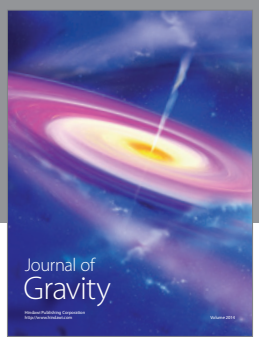

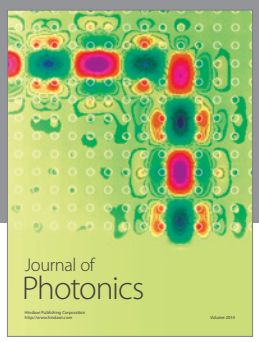

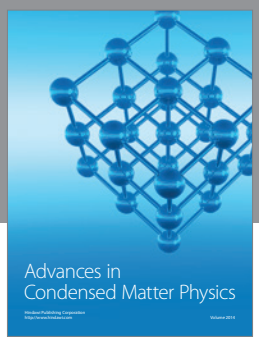

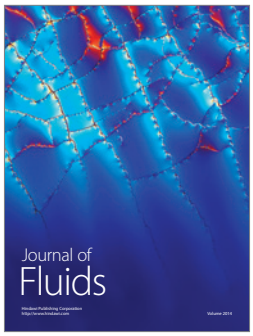

Hindawi
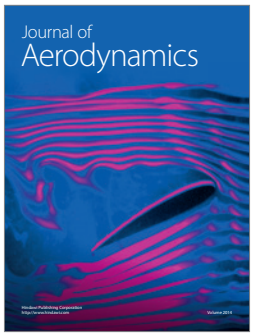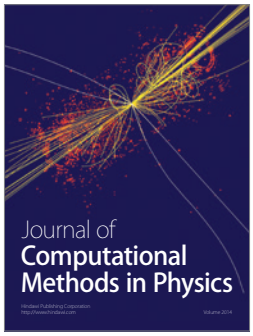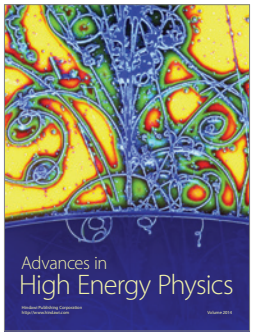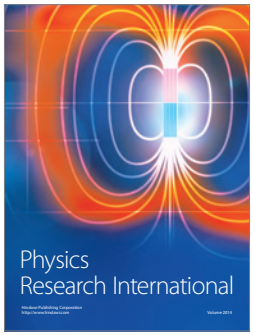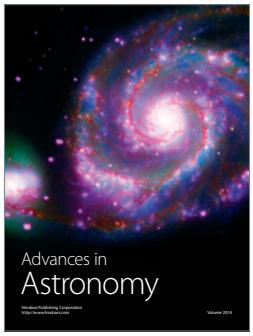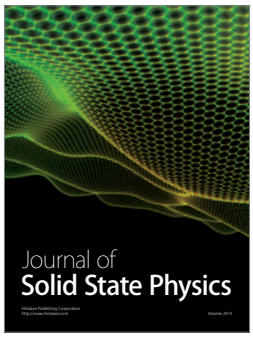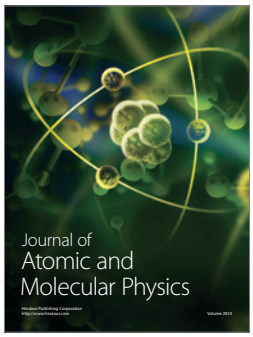
Submit your manuscripts at
http://www.hindawi.com